



Appl. Statist. (2019)
68, Part 1, pp. 29–49

Projecting UK mortality by using Bayesian generalized additive models

Jason Hilton, Erengul Dodd, Jonathan J. Forster and Peter W. F. Smith

University of Southampton, UK

[Received January 2018]

Summary. Forecasts of mortality provide vital information about future populations, with implications for pension and healthcare policy as well as for decisions made by private companies about life insurance and annuity pricing. The paper presents a Bayesian approach to the forecasting of mortality that jointly estimates a generalized additive model (GAM) for mortality for the majority of the age range and a parametric model for older ages where the data are sparser. The GAM allows smooth components to be estimated for age, cohort and age-specific improvement rates, together with a non-smoothed period effect. Forecasts for the UK are produced by using data from the human mortality database spanning the period 1961–2013. A metric that approximates predictive accuracy is used to estimate weights for the ‘stacking’ of forecasts from models with different points of transition between the GAM and parametric elements. Mortality for males and females is estimated separately at first, but a joint model allows the asymptotic limit of mortality at old ages to be shared between sexes and furthermore provides for forecasts accounting for correlations in period innovations.

Keywords: Age–period–cohort; Bayesian analysis; Forecasting; Generalized additive models; Mortality

1. Introduction

The future level of mortality is of vital interest to policy makers and private insurers alike, as lower mortality results in greater expenditure on pension payments and higher social care spending. Individuals are living longer because of improved mortality conditions and will reach higher ages in greater number as the post-war baby boom cohort ages, and thus forecasts of mortality at the oldest ages are becoming more important. However, these remain challenging to produce, as the available mortality data at these ages are sparse and concentrated in the most recent years. The work of Dodd *et al.* (2018a) in producing the 17th iteration of the *English Life Tables* provided a methodology for mortality estimation that combines smoothing based on generalized additive models (GAMs) (Wood, 2006) at the youngest ages with a parametric model at older ages. This paper extends this approach to a forecasting context and introduces period and cohort effects, producing fully probabilistic mortality projections within a Bayesian framework.

2. Mortality forecasting

2.1. Mortality rates

The raw materials for stochastic mortality forecasts are data on the number of deaths d_{xt} in year t and age last birthday x , and matching population counts P_{xt} derived from census data

Address for correspondence: Jason Hilton, Centre for Population Change, University of Southampton, Highfield, Southampton, SO17 1BJ, UK.
E-mail: J.D.Hilton@soton.ac.uk

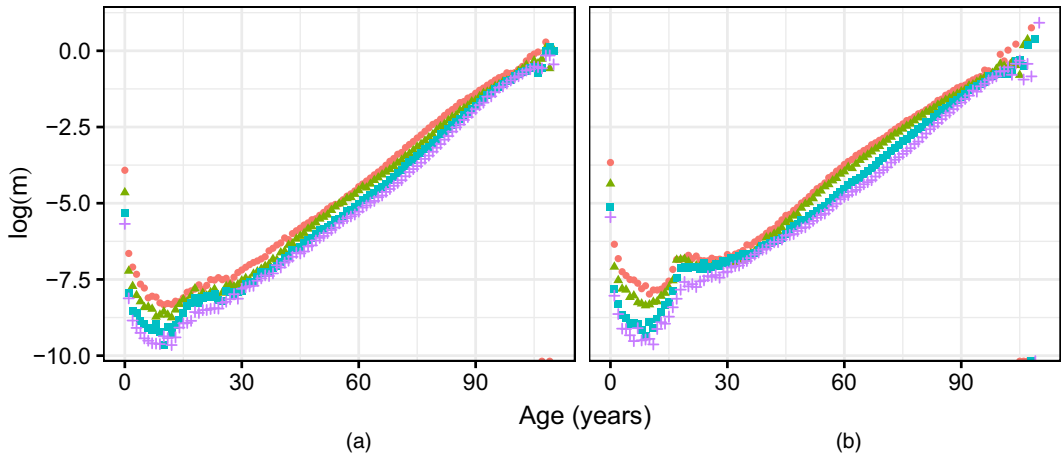


Fig. 1. Log-mortality rates for the UK for selected years for (a) males and (b) females (source: Human Mortality Database (2018)): ●, 1961; ▲, 1981; ■, 2001; +, 2013

adjusted for births, deaths and migration in the intervening period. The appropriate exposures to risk, which are needed for the calculation of mortality rates, can be estimated from these population counts. Most often, the estimated mid-year population totals $P_{x(t+0.5)}$ are used to approximate exposures R_{xt} , directly, over the whole year under the assumption that births, deaths and migrations occur uniformly throughout the year.

The observed deaths rates d_{xt}/R_{xt} for the UK for the years 1961, 1981, 2001 and 2013 are displayed in Fig. 1, based on data taken from the human mortality database (Human Mortality Database, 2018). The human mortality database uses a more sophisticated method of approximating exposure to risk than that described above, accounting for the distribution of deaths within single years of age (Wilmoth *et al.*, 2017). The mortality rates plotted can be seen to decrease with time, and consistently to increase with age beyond early adulthood, as might be expected. The empirical rates appear volatile at higher ages where there are fewer survivors and therefore less data.

The central mortality rate, which is the quantity which we wish to estimate and forecast, is defined as

$$m_{xt} = E[d_{xt}]/R_{xt}. \quad (1)$$

This is equal to the force of mortality or hazard of death $\mu(x)$ within the year and age group under the assumption that the force of mortality is constant over that interval. Thatcher *et al.* (1998) and Keyfitz and Caswell (2005) have provided more detail on the exact relationship between these quantities.

2.2. Models of mortality

A large part of the existing literature on stochastic mortality modelling has developed from the work of Lee and Carter (1992). This approach models the log-mortality rate $\log(m_{xt})$ by using an age-specific term α_x , giving the mean mortality rate for each age x , and a bilinear term $\beta_x \kappa_t$, where the κ -vector describes the overall pace of mortality decline, whereas the β -coefficients describe how this decline varies by age, so that

$$\log(m_{xt}) = \alpha_x + \beta_x \kappa_t. \quad (2)$$

This reduces the complexity of the forecasting problem, as only the κ -component varies over time. This can be modelled by using standard Box–Jenkins methods (most often a random walk with drift), which also provide for measures of forecast uncertainty.

The simplicity of the Lee–Carter model has led to a large range of other adjustments and extensions. Brouhns *et al.* (2002), for example, estimated the parameters through maximization of a Poisson likelihood for the observed deaths rather than working with a Gaussian likelihood on the log-rates, as in Lee and Carter (1992). Renshaw and Haberman (2003a), in contrast, included multiple bilinear age–period terms to capture a greater proportion of the total variation than is possible with a single term.

Renshaw and Haberman (2006) went further by adding a cohort term $\beta_x^{(2)}\gamma_{t-x}$ to allow for differences in mortality by year of birth. Models that include cohort terms are attractive as in some countries, and notably in the UK, cohort effects are prevalent in the underlying mortality data, possibly reflecting the different life experiences and lifestyle habits of those born in different periods (Willets, 2004; Cairns *et al.*, 2009). Standard age–period–cohort (APC) models can therefore capture such characteristics of the data but, given the linear dependence in such models (in that $c = t - x$, with c indexing cohort), identifying constraints are needed for fitting. APC models are widely used in the field of cancer research to make predictions of future cancer rates (e.g. Møller *et al.* (2003)).

The work of Cairns and collaborators (Cairns *et al.*, 2009; Dowd *et al.*, 2010) describes a family of models where mortality is modelled through sums of terms of the form $\beta_x\kappa_t\gamma_{t-x}$, where β_x refers to age effects, κ_t to period effects and γ_{t-x} to cohort effects. Any of these elements may be constant or deterministic in particular models, and so the Lee–Carter and APC models are incorporated as special cases. The in-sample and forecasting performance of these models were assessed against a number of criteria in Cairns *et al.* (2009). A notable finding was the lack of robustness of many of the models that were investigated that included cohort effects; in particular, parameters in such models were found to be sensitive to the fitting period. Furthermore, Palin (2016) has identified some concerns regarding potentially spurious quadratic patterns in cohort effects in several of the models that were discussed above, caused by variation in mortality improvement rates by age being captured in the cohort effect.

Renshaw and Haberman (2003b) identified commonalities between the Lee–Carter model and their generalized linear model approach to mortality modelling focusing on mortality reduction factors. Instead of modelling declines in mortality by using a bilinear term $b_x\kappa_t$, however, Renshaw and Haberman included a term $b_x t$ that is linear in time, simplifying the fitting process. The b_x -parameters now represent age-specific mortality improvements, where improvements are defined as differences in log-mortality. In a similar vein, and building on the cohort enhancement proposed by Renshaw and Haberman (2006), an APC model for improvements has been developed by the Continuous Mortality Investigation (2016). However, this forces a deterministic convergence to user-specified long-term rates of mortality improvement rather than using time series methods for forecasting. Richards *et al.* (2017), however, have provided full stochastic forecasts by using the APC for improvements model by fitting time series models to the period and cohort effects, and also found that this model fits the data better in sample than either the APC or Lee–Carter models.

The smoothing of mortality rates is important in forecasting applications to avoid roughness in the age profile of log-mortality due to random variation being perpetuated into the future. Various smoothing models have thus been proposed. Hyndman and Ullah (2007) approached the problem of mortality forecasting from within the functional data paradigm. From a different perspective, Currie *et al.* (2004) fitted a two-dimensional P -spline to mortality and produced forecasts by extending the spline into the future. The penalization of differences in the basis

function coefficients that was used in the P -spline method to ensure smoothness in sample also provides for extrapolation. Although this model fits the data well, forecasts that are wholly dependent on extrapolation from splines are likely to be oversensitive to data and trends at the forecast origin.

Bayesian methods are also increasingly being employed for mortality forecasting to incorporate prior knowledge about underlying processes, and to provide distributions of future mortality risk accounting for multiple sources of uncertainty. Girosi and King (2008) demonstrated methods for mortality forecasting within a Bayesian framework that allow for smoothing the underlying data together with borrowing strength across regions, as well as jointly forecasting cause-specific mortality. Wiśniowski *et al.* (2015) used the Lee–Carter method for all three components of demographic change (fertility, mortality and migration), again using Bayesian methods to obtain predictive probability distributions.

The method that is developed in this paper combines elements of many of the approaches above, including allowing for smooth functions of age and cohort, while providing stable estimates of mortality at extreme ages and avoiding some of the problems that are caused by lack of robustness in parameter estimation that was discussed above. The model also shares some features with the APC for improvements model of Richards *et al.* (2017), particularly in the structure of the main part of the model. However, there are some significant points of difference; the model that is described here applies to the entire age range and adopts a Bayesian approach to account for all sources of uncertainty.

2.3. Structure

The remainder of the paper is structured as follows: Section 3 sets out the features of the model that are used in later sections. Section 4 details the data that are used and the estimation procedure. Section 5 presents the posterior distributions of the GAM components and provides predictive distributions for log-rate forecasts, and Section 6 displays posterior distributions combined over several alternative models on the basis of in-sample predictive performance, using the method of Yao *et al.* (2018). Section 7 presents an alternative model where the sexes are fitted jointly, whereas Section 8 compares out-of-sample performance of the single-sex and joint models, using the years 2004–2013. Section 9 contrasts forecasts from the joint model with those made by the UK Office for National Statistics (ONS) (Office for National Statistics, 2016), and the final section offers some conclusions and directions for future work.

The programs that were used to analyse the data can be obtained from

<http://wileyonlinelibrary.com/journal/rss-datasets>

3. Model description

3.1. Bayesian generalized additive models

GAMs provide a flexible framework for modelling outcomes where the functional form of the response to covariates is not known with certainty but is expected to vary smoothly. The general form for such models is as follows (Wood, 2006):

$$g\{E(y_i)\} = \mathbf{x}_i\boldsymbol{\theta} + s_1(x_{i1}) + s_2(x_{i2}) + \dots$$

Here, the expectation of the outcome y , possibly transformed by link function $g(\cdot)$, is modelled as the sum of a purely parametric part $\mathbf{x}_i\boldsymbol{\theta}$ and a number of smooth functions of covariates $s(\cdot)$. Various possible choices exist for the implementation of the individual smooth functions, but P -splines are chosen in this case. P -splines are appealing because they are defined in terms of

strictly local basis functions, with the domain of each function defined by a set of knots spread across the covariate space (Wood, 2016). Following the Bayesian P -splines approach of Lang and Brezger (2004), prior distributions are used to represent a belief that adjacent P -spline covariates β will be close to one another. Multivariate normal prior distributions are used, with the covariance matrix constructed from two matrices: A providing a penalty on the first differences of the vector of coefficients β , and B penalizing the null space of A ensuring that the resulting prior is proper (Wood, 2016):

$$s(x) = \beta^T \mathbf{b}(x),$$

$$\beta \sim \text{MVN} \left\{ \mathbf{0}, \left(\frac{1}{\sigma_A^2} A + \frac{1}{\sigma_B^2} B \right)^{-1} \right\}. \quad (3)$$

3.2. Generalized additive models for mortality forecasting

The method of mortality forecasting that is developed in this paper fits a GAM to the majority of the age range, while applying separate parametric models to older age groups and to infants. This enables a flexible but smooth fit where the data allow and imposes some structure on the model where data are sparse, particularly at very high ages. Deaths d_{xt} are considered to follow a negative binomial distribution parameterized in terms of the mean, which in this case is equal to the product of the relevant exposure E_{xt} and expected death rate m_{xt} . The dispersion ϕ captures additional variance relative to the Poisson distribution:

$$d_{xt} \sim \text{NegBinomial}(E_{xt}m_{xt}, \phi),$$

$$p(d_{xt}|m_{xt}, E_{xt}, \phi) = \frac{\Gamma(d_{xt} + \phi)}{d_{xt}! \Gamma(\phi)} \left(\frac{E_{xt}m_{xt}}{E_{xt}m_{xt} + \phi} \right)^{d_{xt}} \left(\frac{\phi}{E_{xt}m_{xt} + \phi} \right)^{\phi}.$$

An APC GAM for the log-mortality improvement ratios $\log(m_{xt}/m_{x(t-1)})$ could be expressed with P -spline-based smooth functions for age and cohort improvements, and an additional period component κ :

$$\log \left(\frac{m_{xt}}{m_{x(t-1)}} \right) = s_{\beta}(x) + s_{\gamma}^*(t - x) + \kappa_t^*. \quad (4)$$

An equivalent expression of this model can be made in terms of mortality rates rather than mortality log-improvement-ratios

$$\log(m_{xt}) = s_{\alpha}(x) + s_{\beta}(x)t + s_{\gamma}(t - x) + \kappa_t, \quad (5)$$

with the cohort and period terms now accumulated versions of their equivalents in equation (4). This is the model that is used in the estimation process. There are now two smooth functions of age: $s_{\alpha}(x)$, which describes the underlying shape of the log-mortality curve, and $s_{\beta}(x)$, which describes the pattern of (linear) mortality improvements with age. Knots are spaced at regular intervals in both the age and the cohort direction (every 4 years), with three knots placed outside the range of the data at either end of the age range, enabling a proper definition of the P -spline at the edge of the data.

In common with other models involving age, period and cohort elements, constraints are needed to identify the different effects because of the linear relationship between the three components. For this, the cohort component $s_{\gamma}(t - x)$ is constrained so that the first and last components are equal to 0, and the sum of effects over the whole range of cohorts is 0. The period components κ_t are similarly constrained to sum to 0 and to display zero growth over the fitting period. The full set of constraints is thus

$$\begin{aligned} \sum_{t=1}^T \kappa_t &= 0, & \sum_{t=1}^T t\kappa_t &= 0, \\ \sum_{c=1}^C s_\gamma(c) &= 0, & s_\gamma(1) &= 0, & s_\gamma(C) &= 0, \end{aligned} \quad (6)$$

with C here indicating the most recent cohort and T the latest year. These constraints ensure that linear improvements in mortality with time are estimated as part of the $s_\beta(x)$ term.

For older ages, a parametric model is adopted because of the sparsity of the data in these regions—the additional structure that is provided by specifying a parametric form guards against overfitting and instabilities in this age range:

$$m_{xt} = \frac{\exp(\beta_0^{\text{old}} + \beta_1^{\text{old}}x + \beta_2^{\text{old}}t + \beta_3^{\text{old}}xt)}{1 + \exp(\beta_0^{\text{old}} - \log(\psi) + \beta_1^{\text{old}}x + \beta_2^{\text{old}}t + \beta_3^{\text{old}}xt)} \exp\{s_\gamma(t - x) + \kappa_t\} \quad \forall x : x \geq x_{\text{old}}. \quad (7)$$

A logistic form is used, allowing mortality rates to tend towards a constant ψ as age increases, as in the model in Beard (1963). Such a pattern in mortality at the population level has some theoretical justification, as it can result when heterogeneity (‘frailty’) is applied to rates that follow a log-linear Gompertz mortality model at the individual level, and this frailty is assumed to be distributed among the population according to a gamma distribution (Vaupel *et al.*, 1979). In the life table context, Dodd *et al.* (2018a) found that the logistic form performed better than the log-linear equivalent when assessed by using cross-validation techniques. Linear age and time effects are included in the old age model, together with an interaction term, and the cohort and period effects are held in common with the model that is applied to younger ages and are applied multiplicatively to the logistic model.

Constraints are also applied to the parameters of the old age model to ensure that the derivative of the parametric part of the model with respect to age (ignoring the period and cohort effects) is never less than 0; this reflects our prior belief that mortality should not decrease with age after middle age. The constraints that are required are as follows, with H describing the most distant time for which forecasts are desired:

$$\left. \begin{aligned} \beta_1^{\text{old}} &> 0, \\ \beta_2^{\text{old}} &< 0, \\ \beta_3^{\text{old}} &> -\beta_1^{\text{old}}/H. \end{aligned} \right\} \quad (8)$$

Infant mortality is also excluded from the GAM, as it behaves differently from mortality at other ages. The model for infants is given a similar structure to the old age model, except that the period effect κ_t is excluded, as variation in infant mortality with time does not appear to follow the same pattern as it does over the rest of the age range:

$$\log(m_{0t}) = \beta_1^0 + \beta_1^0 t + s_\gamma(t). \quad (9)$$

The period-specific effects κ_t in equations (5) and (7) are common across ages and capture deviations from the linear trend that is described by the smooth improvements s_β . These effects are not modelled as smooth, as they may capture effects such as weather conditions or infectious disease outbreaks that would not be expected to vary smoothly from year to year. The innovations in these period effects ϵ are given a normal prior with variance σ_κ , so that

$$\begin{aligned} \kappa_t &= \kappa_{t-1} + \epsilon_t, \\ \epsilon_\kappa &\sim N(0, \sigma_\kappa^2). \end{aligned} \quad (10)$$

However, these effects are constrained to identify the APC model, so we need to account for this by conditioning on the two period constraints that are given in equation (6). This is achieved by transforming the ϵ -parameters by using a matrix Z , constructed so that the final $T - 2$ parameters remain unchanged, but the first two transformed parameters will equal 0 if the constraints on the cumulative sum of the ϵ -series hold (see the on-line appendix). The resulting vector η has a multivariate normal distribution

$$\begin{aligned}\eta &= Z\epsilon, \\ \eta &\sim \text{MVN}(\mathbf{0}, ZZ^T \sigma_\kappa^2).\end{aligned}\tag{11}$$

A distribution conditioning on the first two elements of η , denoted η^\dagger , equalling 0 can be obtained by using standard results for the multivariate normal distribution. This conditional prior on η^* (which contains the last $T - 2$ elements of η) is the distribution that is used for sampling, and the full set of values of ϵ can then be recovered deterministically:

$$\left. \begin{aligned}\eta &= \begin{pmatrix} \eta^\dagger \\ \eta^* \end{pmatrix}, \\ \eta^* | (\eta^\dagger = \mathbf{0}) &\sim N(0, \Sigma_{**} - \Sigma_{*\dagger} \Sigma_{\dagger\dagger}^{-1} \Sigma_{\dagger*}), \\ \Sigma &= ZZ^T \sigma_\epsilon^2, \\ \epsilon &= Z^{-1} \begin{pmatrix} \mathbf{0} \\ \eta^* \end{pmatrix},\end{aligned}\right\}\tag{12}$$

where subscripts on the covariance matrices indicate partitions, so $\Sigma_{*\dagger}$ is the submatrix of Σ with rows corresponding to η^* and columns to η^\dagger . For forecasts, innovations of the period coefficients are unconstrained and so have independent normal distributions with variance σ_κ^2 .

The same method is used to define a distribution for the innovations in the basis functions coefficients for the cohort spline, accounting for the cohort constraints in equation (6) and replacing the prior in expression (3). In contrast with the period effects, however, the transformation matrix that is used accounts for the fact that the constraints apply to the resulting smooth function and not the coefficient values themselves. Knots for the basis functions of the cohort smooth are evenly spaced along the range of cohorts to be estimated, so forecasts of future cohort values can be obtained by drawing new coefficient innovations from the normal distribution with mean 0 and variance σ_γ^2 which replaces σ_A^2 and σ_B^2 for this effect. Full details are given in the on-line appendix.

Priors for the model hyperparameters are generally vague, although not completely uninformative:

$$\begin{aligned}\beta^{\text{old}} &\sim N(0, 100), \\ \beta^0 &\sim N(0, 100), \\ \sigma_A &\sim N_+(0, 100), \\ \sigma_B &\sim N_+(0, 100), \\ \sigma_\kappa &\sim N_+(0, 100), \\ \sigma_\gamma &\sim N_+(0, 100), \\ \phi &\sim U(-\infty, \infty), \\ \psi &\sim \text{LogNormal}(0, 1).\end{aligned}$$

The adoption of weakly informative priors aims to capture something about the expected scale and location of the parameters in question; this aids convergence of the Markov chain Monte

Carlo samples, but with reasonable amounts of data should not affect the final inference to any great extent (Gelman *et al.*, 2014). The scale of the data and covariates is also important in determining the interpretation of these priors; the use of standardized age and time indices means that regression coefficients are unlikely to take large values. The use of the addition symbol as a subscript appended to the normal distribution, N_+ , indicates that only the positive part of the normal distribution is used and therefore refers to a half-normal distribution.

4. Estimation

Samples from the posterior distributions of the parameters and rates were drawn by using Hamiltonian Monte Carlo sampling and specifically using the *stan* software package (Stan Development Team, 2015). *stan* and its interface in the R programming language (R Core Team, 2017) allows the construction of a Hamiltonian Monte Carlo sampling ‘no U-turns sampler’ (Hoffman and Gelman, 2014) from a simple user specification of the Bayesian model to be estimated. The code that is required to fit the model is also available from <https://github.com/jasonhilton/mortality-bgam>. Hamiltonian Monte Carlo sampling is a special case of the more general Metropolis–Hastings algorithm for Markov chain Monte Carlo sampling and uses the derivatives of the log-posterior with respect to the parameters of interest in the sampling process, often enabling the posterior to be traversed much more quickly than under standard methods (Neal, 2010). The model was fitted using human mortality database data for the UK from 1961 to 2013 (Human Mortality Database, 2018). The first five cohorts (those born before 1856) were excluded, as exposures are very low for these groups. Four parallel chains were constructed, each with 8000 samples, and the first half of each chain was used as a warm-up period (during which *stan* tunes the algorithm to reflect the characteristics of the posterior best) and discarded. Parallel chains were used to assess convergence to the posterior distribution better; the diagnostic measure that was advocated by Gelman and Rubin (1992) indicates that all parameters have converged to an acceptable degree. The 16000 post-warm-up samples were ‘thinned’ by a factor of 4 by discarding three values in four to avoid excessive memory usage, leaving 4000 posterior samples for inference for each model.

5. Initial results

Some preliminary results are displayed in this section, conditionally on a particular choice for the point of transition between the GAM to the parametric old age model. Fitting a similar model to ONS data for England and Wales for 2010–2012, Dodd *et al.* (2018a) found by using cross-validation methods that the most probable points of transition were age 91 for females and 93 years for males. Samples were obtained for models using these transition points, and the posterior distributions of the parameters of the GAM model are given in Figs 2 and 3 for males and females respectively. The colour scheme in these plots identifies intervals containing various proportions of the posterior density, so that the darkest represents the central 2% interval, whereas 90% of the posterior density is contained between the lightest bands. The distributions of mortality improvement rates for both males and females display greater uncertainty at younger ages where there are fewer deaths. As might be expected, uncertainty for cohort effects increases for the oldest and most recent cohorts, as these have the fewest data points. Note that it is the differenced cohort and period effects ($s_\gamma^*(t - x)$ and κ_t^* from equation (4)) that are plotted rather than their summed equivalents.

Differences between the sexes are most notable in the age-specific component, for which the accident hump for young males is more prominent, and in the improvement rates, for which males

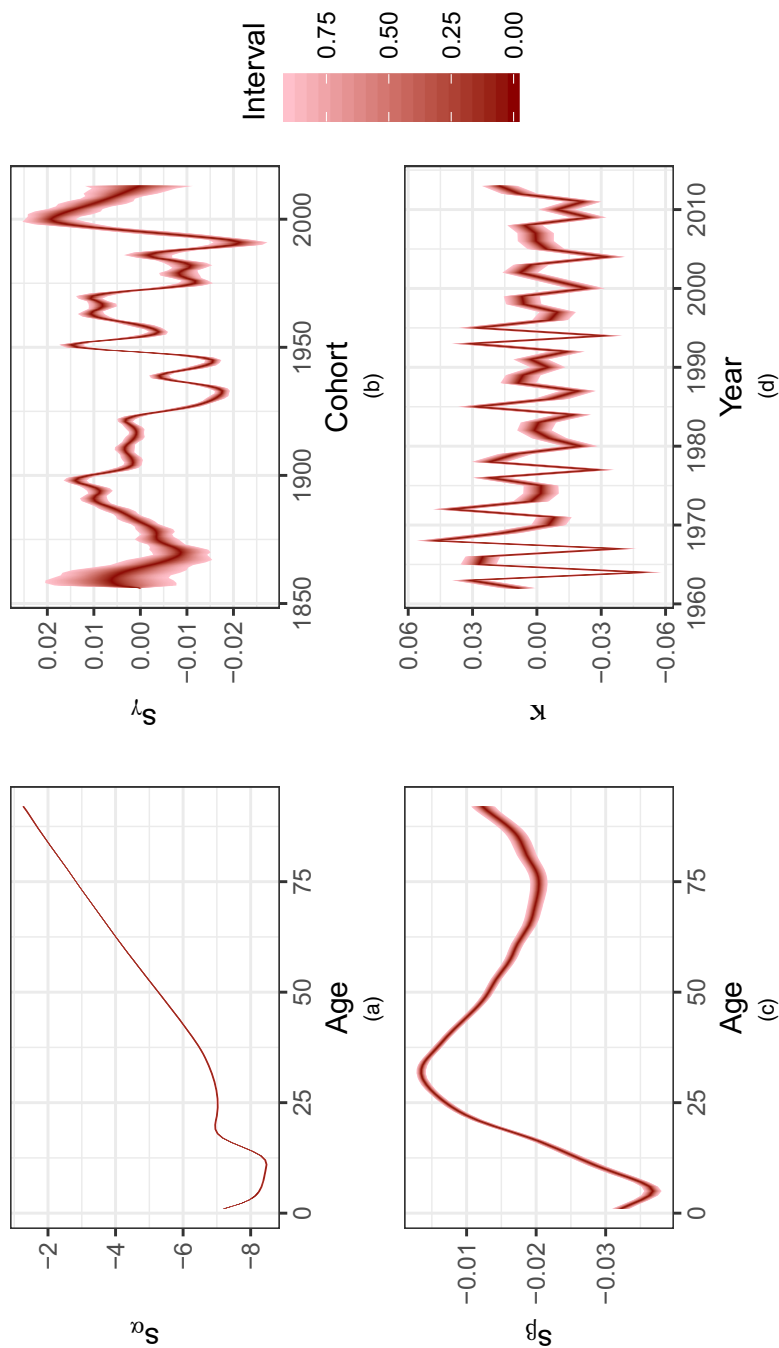


Fig. 2. GAM components, males, transition point 93 years: (a) age; (b) cohort; (c) improvement; (d) period

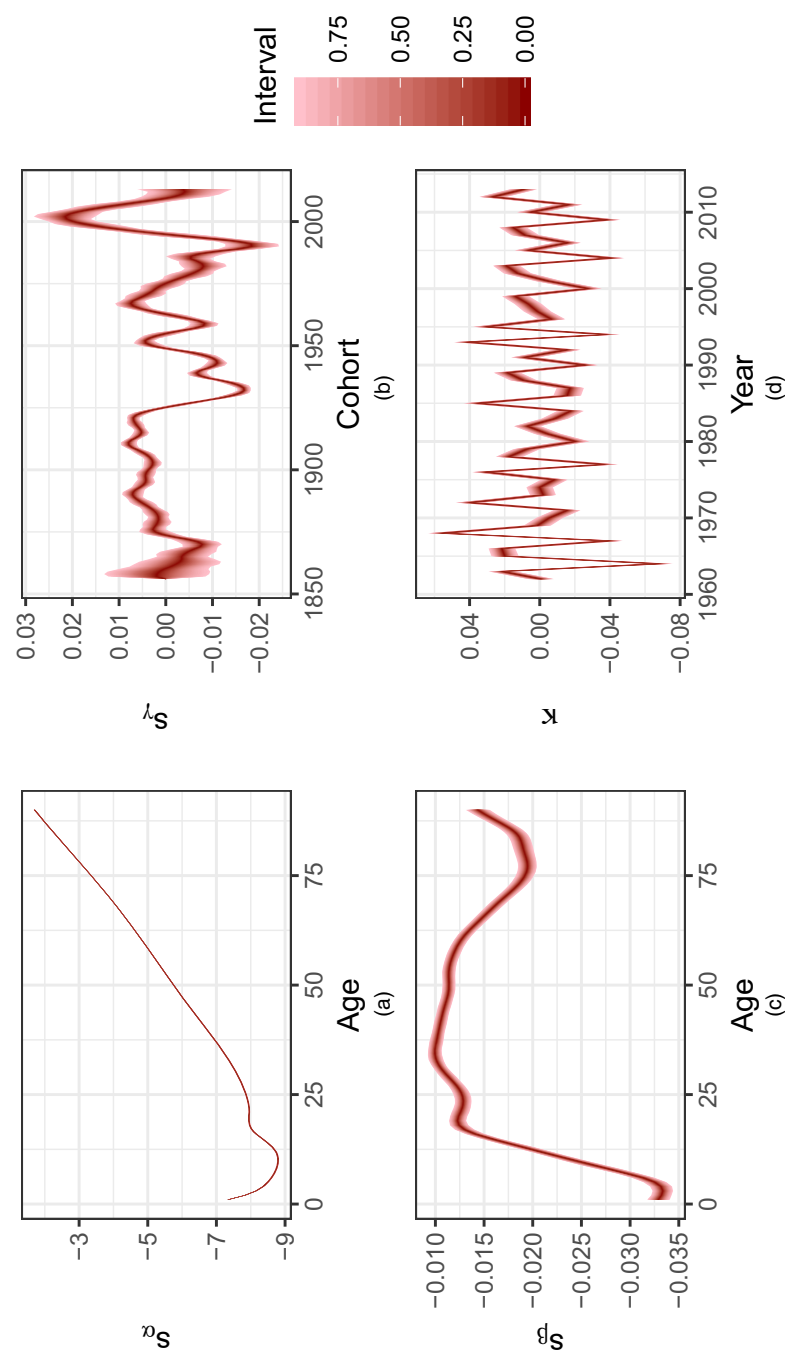


Fig. 3. GAM components, females, transition point 91 years: (a) age; (b) cohort; (c) improvement; (d) period

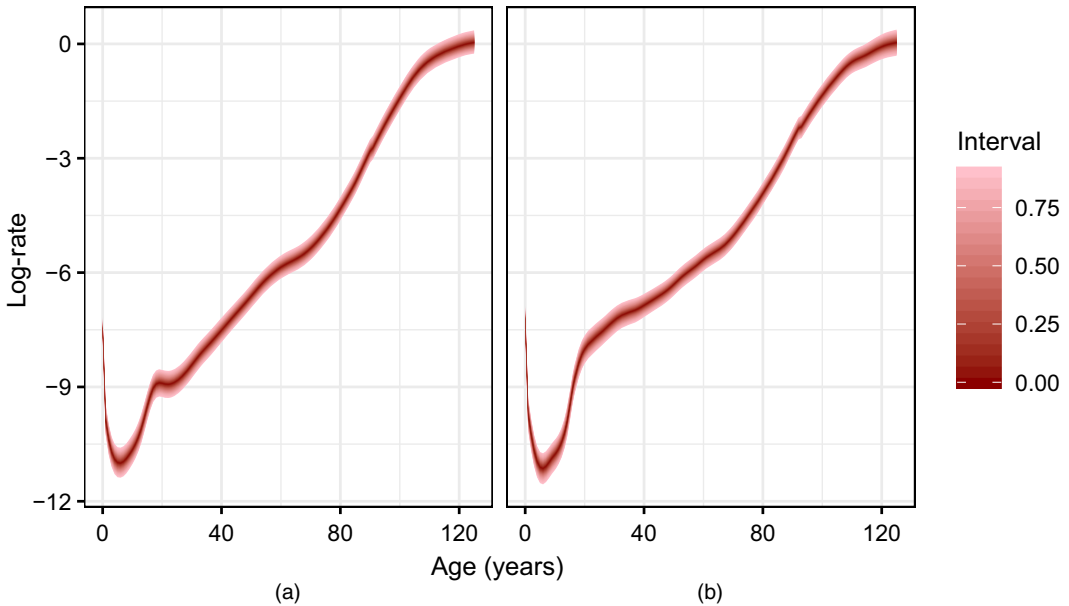


Fig. 4. Predictive distribution of log-rates with single points of transition, 2063: (a) females; (b) males

show lower rates of improvement than females in their late 20s. Cohort and period contributions to mortality decline show similar but not identical patterns for each sex.

Posterior distributions for log-rates generated from this model fit the data relatively closely. However, Fig. 4 displays forecasts of log-rates at 50 years into the future, which, although appearing reasonable, contain small discontinuities at the point of transition between the GAM and the parametric model. The discontinuity is particularly evident in the forecast for males. This suggests that some sort of averaging over or combination of models using different transition points might be advisable.

6. Transition points and model stacking

The choice that is made regarding the age at which the model transitions from the GAM (which is used over the majority of the age range) to the parametric model for old ages is essentially arbitrary; we do not believe that there is a switch between data-generating processes at some point x_{old} , but rather that the task of predicting mortality is better served by two models. There is thus no ‘true’ value for the point of transition, and decisions regarding transition should be governed by model performance. The methodology that was used in the latest *English Life Tables* (Dodd *et al.*, 2018a) used cross-validation to obtain posterior weights over a set of models M defined by K different points of transition, based on mortality data from 2010 to 2012. In that analysis, age 91 for females and 93 years for males are the most probable points of transition, and the final predictive distribution was obtained by averaging over models using the calculated weights. However, the model that is described here differs from that used in Dodd *et al.* (2018a) in that it varies in time and applies to a period spanning many years, so the question of the distribution of the transition between the parametric model and the GAM must be revisited.

Separate models were therefore estimated for transition points ranging from 80 to 95 years, and their accuracy was assessed by using the *leave-one-out information criterion* (LOOIC),

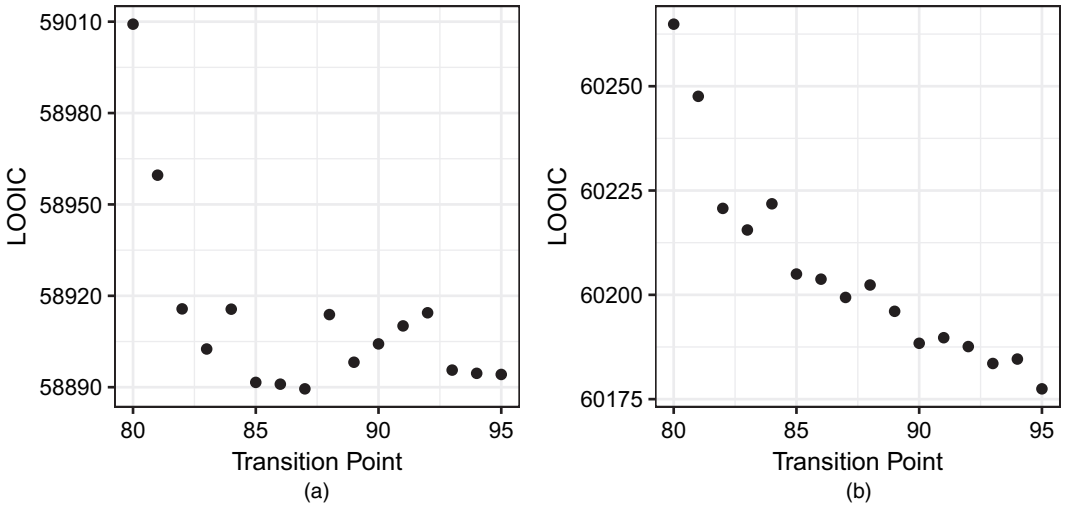


Fig. 5. LOOIC values for models by using different transition points: (a) females; (b) males

developed by Vehtari *et al.* (2016). The LOOIC is a measure of how well we might expect a model to perform in predicting a data point without including it in the data that are used to fit the model. It is based on an approximation of the leave-one-out log-pointwise predictive density $\sum_{i=1}^n \log\{p(y_i|y_{-i})\}$, where the y_{-i} subscript indicates a data set excluding the i th observation, θ is a vector of parameters and

$$p(y_i|y_{-i}) = \int p(y_i|\theta) p(\theta|y_{-i}) d\theta.$$

Rather than fitting the model n times (once for every data point), Vehtari *et al.* (2016) provided a method for approximating the LOOIC from just one set of posterior samples of the predictive density computed from the full data set, implemented within the `loo` R package. This uses importance sampling to approximate the leave-one-out log-predictive-density, correcting for instabilities caused by the potentially high or infinite variance of some importance weights by fitting a Pareto distribution to the upper tail of the raw weights.

The LOOIC scores for males and females for the models with transition points $k = [80, 81, \dots, 95]$ years are given in Fig. 5. Later cut points tend to be preferred because the greater flexibility of the GAM model gives lower LOOIC values even at relatively high ages, although the absolute differences between the models are small. Models with points of transition above age 95 years are not considered, as this would leave too few data points with which to estimate the old age model effectively.

Although the LOOIC is not a measure of *forecast* performance as such, as it is focused on how the model would perform at predicting data points that are contained within the original data set and does not consider the times at which data points become available, it does provide an indication of how well the models specified reflect the structure of the data.

Following the work by Yao *et al.* (2018), these LOOIC values can be used as the basis for ‘stacking’ the predictive distributions of each model to obtain a distribution which combines models in a principled way, with weights determined by approximate cross-validation performance. Stacking is often used for averaging over point estimates in ensemble models, but Yao *et al.* (2018) extended the approach to apply to combining distributions. More specifically, the

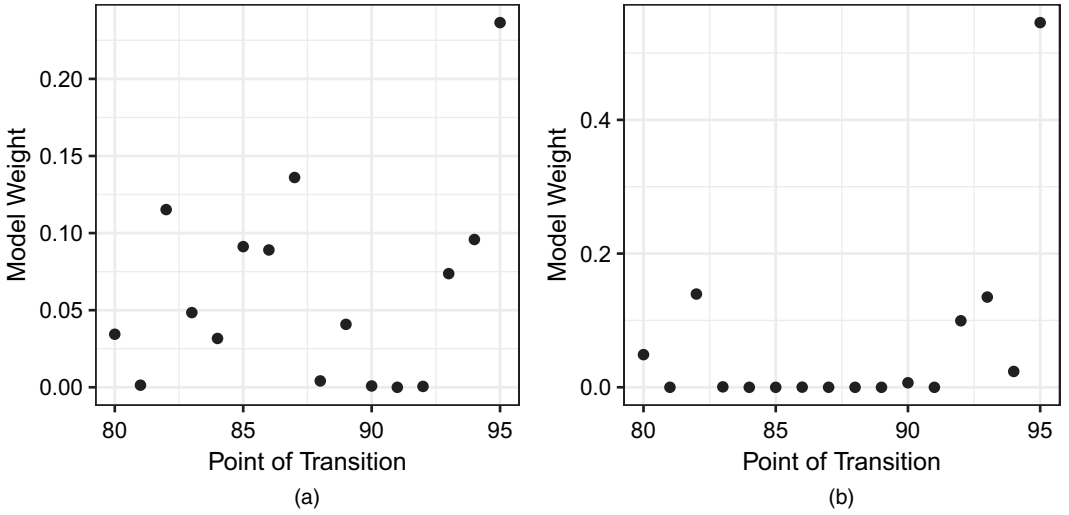


Fig. 6. LOOIC values for models by using different points of transition: (a) females; (b) males

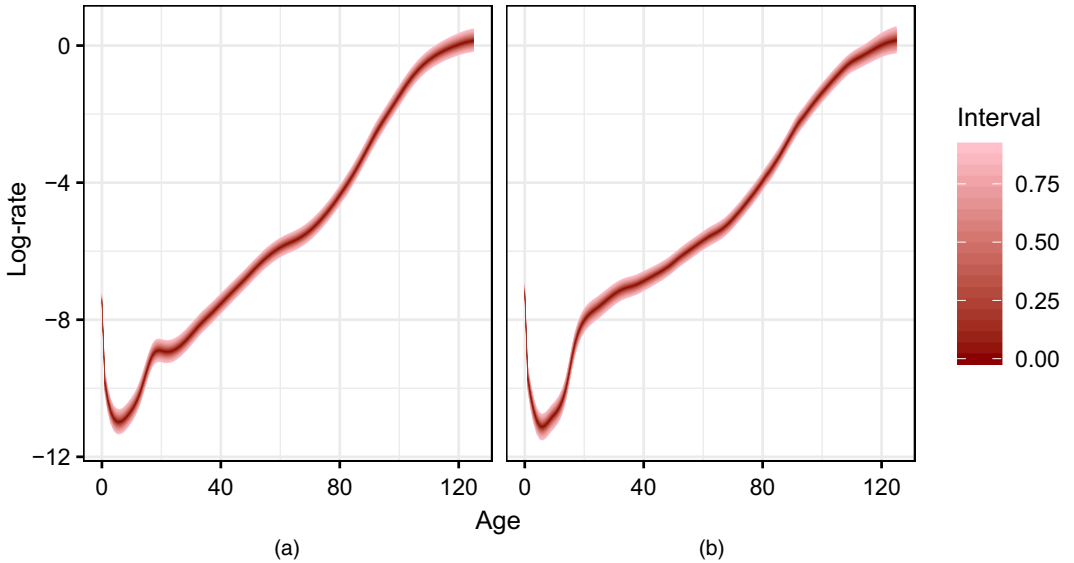


Fig. 7. Stacked forecasts for 2063, single-sex models: (a) females; (b) males

weights \mathbf{w} , elements of which correspond to one of K possible models M_k , are estimated through the solution of the optimization problem

$$\arg \max_{\mathbf{w}} \sum_{i=1}^n \log \left\{ \sum_{k=1}^K w_k p(y_i | y_{-i}, M_k) \right\} \quad \text{subject to } w_k > 0, \sum_{k=1}^K w_k = 1, \quad (13)$$

(Yao *et al.* (2018), page 7), where $p(y_i | y_{-i}, M_k)$ is approximated by using the LOOIC measure described above. The form of the combined predictive distribution is then

$$\hat{p}(\tilde{y} | y) = \sum_{k=1}^K w_k p(\tilde{y} | y, M_k).$$

The estimated model weights are shown in Fig. 6; the greatest individual weight is given to models with the latest points of transitions, reflecting the pattern in the LOOIC measure. Other models with earlier transition points are also given weight, however, reflecting that they perform well at predicting some data points which are not so well estimated by the late transition model.

Samples from the combined posterior predictive distribution were obtained by using the estimated weights by sampling from the posterior distribution that is associated with each model in proportion to its weight. The resulting stacked forecasts are given in Fig. 7; the discontinuities that were seen previously are now smoothed out through the process of taking the weighted combination of distributions.

7. Jointly modelling male and female mortality

In the work that was described above, models for males and females were estimated separately. However, much of what drives the underlying processes of mortality and how it changes over time is likely to be common between sexes. Thus, we may gain from borrowing strength across models and also from explicitly representing covariances between parameters for each sex, as in Wiśniowski *et al.* (2015). Because males tend to die sooner than females, there are fewer data points (i.e. lower total exposure) with which to estimate parameters in the old age model. For this reason, the parameter ψ , representing the asymptote of the logistic function in the old age model, is now shared between sexes.

We also allow the innovations in the period effects κ_t to be correlated, so that joint forecasts can be generated accounting for the fact that, in potential futures where mortality for females is high, it will tend to be high for males as well. The joint distribution for the period innovations for both sexes, conditionally on the constraints, is obtained in a similar way to that for the single-sex models, described in Section 3. Full details are given in the on-line appendix.

As before, LOOIC scores and model weights were obtained for the joint model (Fig. 8). The pattern of LOOIC scores and weights are similar to those for the separate models, with the highest transition point obtaining most weight, but considerable weight also attached to earlier transitions.

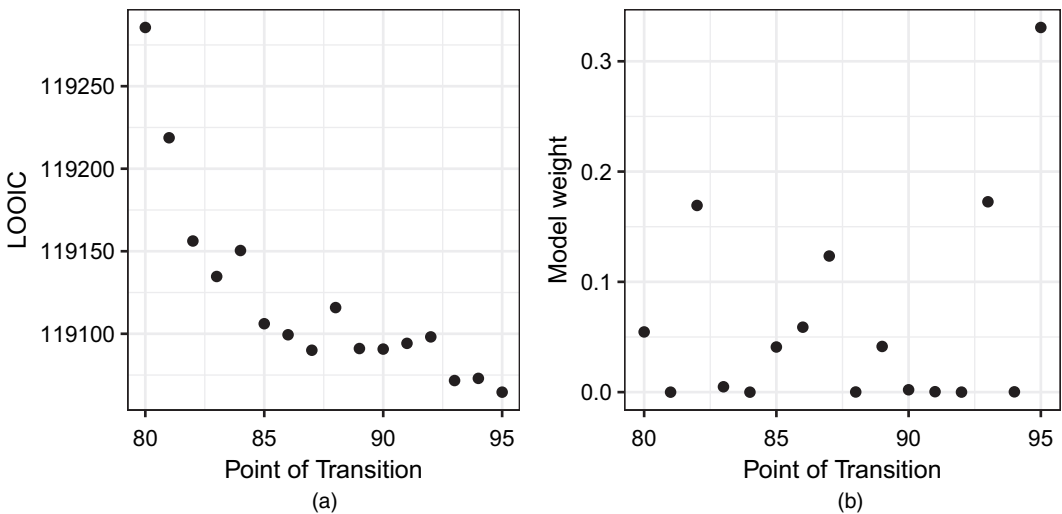


Fig. 8. (a) LOOIC and (b) model weights, joint-sex model

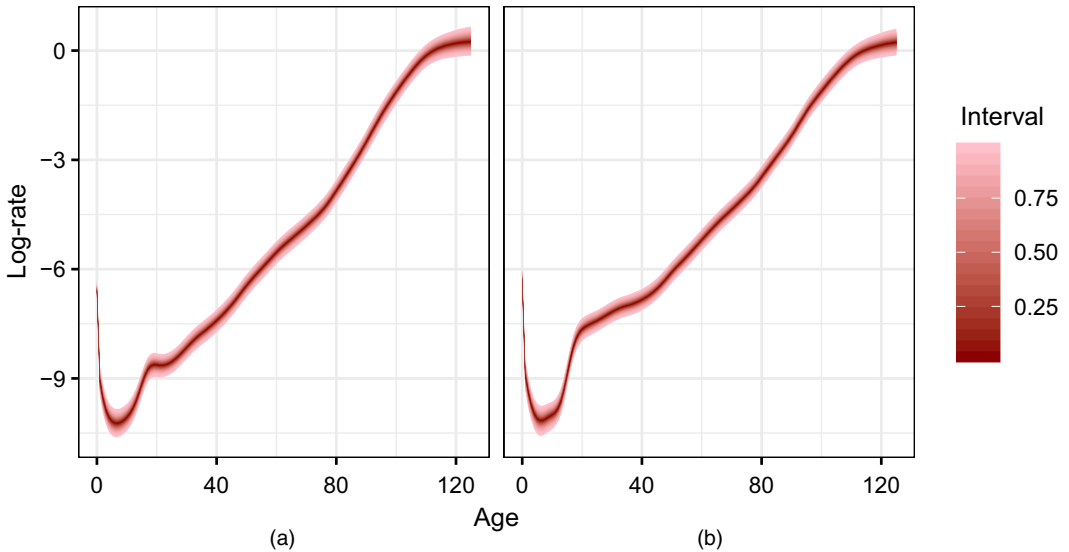


Fig. 9. Stacked forecasts from the joint-sex model, 2038: (a) females; (b) males

Joint forecasts of log-mortality are displayed in Fig. 9. The estimated correlation in the innovations of the period effects (the off-diagonal elements of P) is high—generally above 95%.

8. Model assessment

To assess the robustness and forecasting accuracy of the models that were described above, fitting was conducted on a truncated data set, excluding the years 2004–2013. Robustness was then assessed by comparing posterior means of the main smooth functions estimated on this reduced data set against the same quantities estimated on all the data. Fig. 10 displays such a comparison for males, plotting posterior means for each point of transition and fitting period. Estimates of period and cohort effects are relatively stable, particularly in the interior of the data. Although some differences are evident in the pattern of improvements, the general shape of the curve is notably similar, and the downward shift appears to reflect real increases in the rate of mortality decline after 2003, particularly for younger adults. The shape of the age effect is again very similar, and the differing location of the smooth curve is accounted for by a change in the location of the intercept of the time index in equation (5) for different data periods.

Both the single- and the joint-sex models that were presented above appear to give reasonable forecasts for future mortality. Figs 11 and 12 display predictive distributions and empirical rates for younger and older ages respectively. Comparing the predictive posterior distributions against the observed outcomes, it is evident that, for most of the age range, empirical rates fall within the 90% predictive interval. The exception is young adult males, between the ages of about 15 and 40 years, for whom recent drops in mortality far outpace those seen in the observed data 1961–2003. More formal assessments of forecast performance are difficult, as we observe only one correlated set of outcomes (i.e. male and female log-rates 2004–2013).

Focusing on older ages (Fig. 12), we can see that there are few differences between the predictive distributions of the joint- and single-sex models, and those that are evident occur only at high ages. In part, this may be because the weighting procedure works to select models with

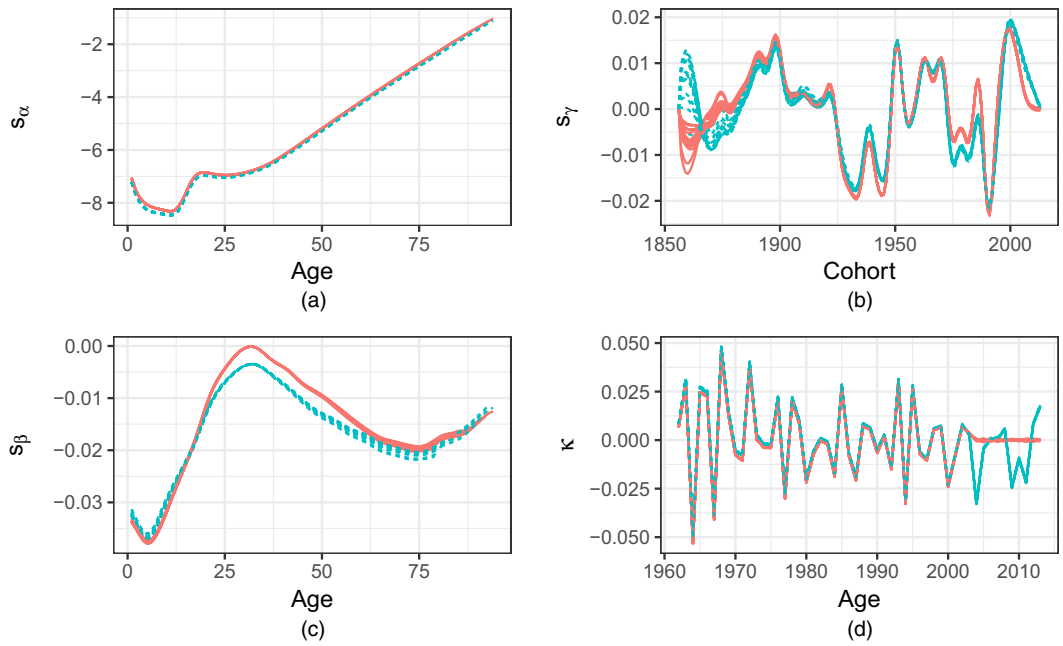


Fig. 10. Comparison of posterior means of GAM components for various fitting periods (—, 1961–2003; —, 1961–2013) and transition points, males: (a) age; (b) cohort; (c) improvement; (d) period

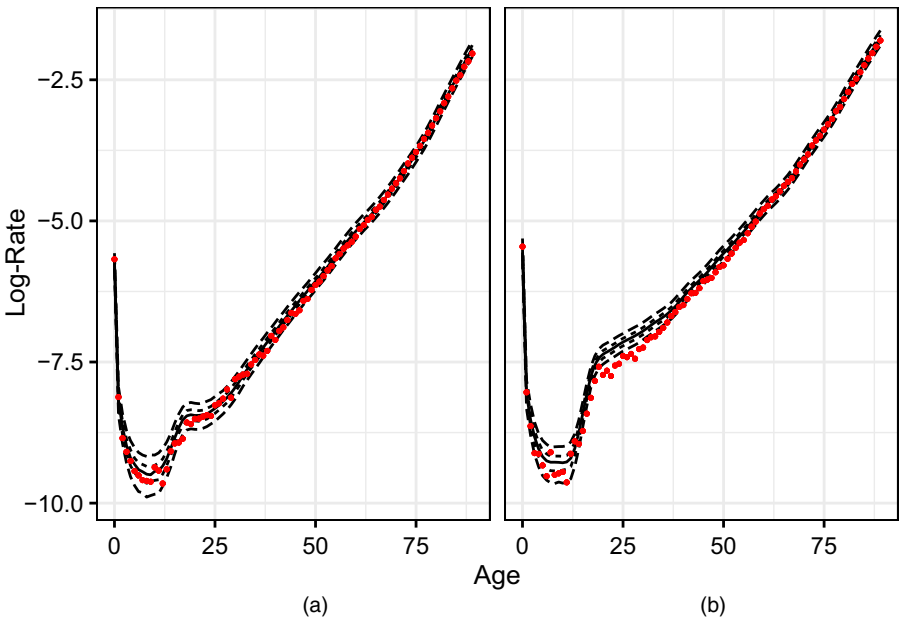


Fig. 11. Comparison of posterior predictive distributions for log-rates against empirical observations, 2013, joint-sex model (—, median; ----, 0.5 percentile; - - -, 0.9 percentile): (a) females; (b) males

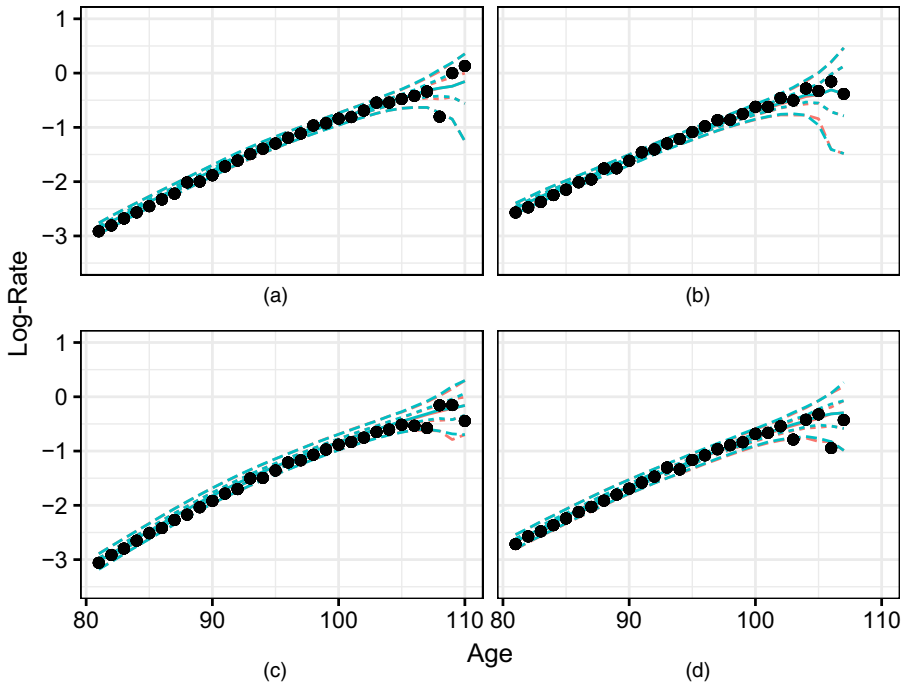


Fig. 12. Comparison of posterior predictive distributions for old-age log-rates against empirical observations, (a), (b) 2008 and (c), (d) 2013, single- (—) and joint-sex (—) models (—, median; ----, 0.5 percentile; - · -, 0.9 percentile): (a), (c) females; (b), (d) males

similar properties. Other considerations may be taken into account when deciding between the two models; the joint model is more parsimonious in that fewer parameters are required to fit it, and it allows for correlations in the paths of mortality by sex to be taken into account. In contrast, the single-sex model is less computationally demanding, particularly with respect to memory, as each sex is fitted and processed separately.

9. Comparison with official projections and variants

The final stacked forecasts from the joint model in the previous section are now compared with forecasts that are produced by the UK ONS in the 2014-based national population projections (NPPs) (Office for National Statistics, 2016). These work with the predicted probabilities of deaths q_x rather than the central mortality rates m_x ; the former represents the probability of dying by age $x + 1$ given that an individual attains age x . Posterior predictive samples of q_{xt} were acquired by using the approximation

$$q_{xt} \approx 1 - \exp(-m_{xt}). \quad (14)$$

As well as the principal ONS projection from the 2014-based NPP, the variant projections involving high and low mortality scenarios have been included, allowing some understanding of how the existing indications of uncertainty resulting from different projection assumptions compare with the fully Bayesian probability distributions.

Fig. 13 shows posterior distributions of log-transformed probabilities of death q_x for a forecast horizon of 25 years for both males and females, together with the equivalent $q_{x+0.5-}$

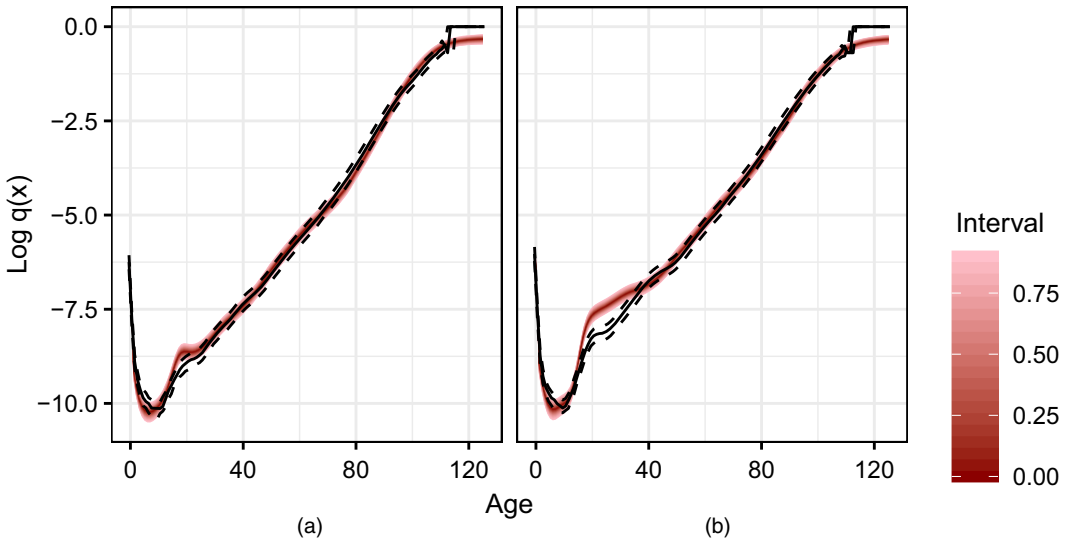


Fig. 13. Forecast log-probabilities of death for 2038 (— — —, ONS variant high; — · — · —, ONS variant low; —, principal ONS variant): (a) females; (b) males

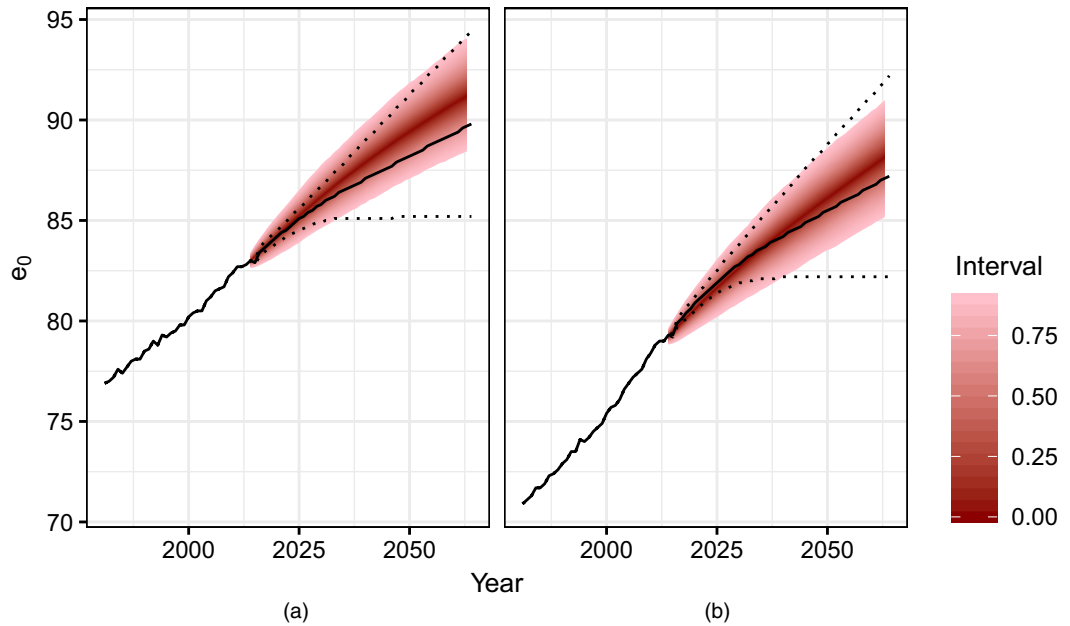


Fig. 14. Forecast life expectancy at birth, ONS NPP and GAM-based forecast (· · · · ·, ONS variant high; · · · · ·, ONS variant low; —, principal ONS variant): (a) females; (b) males

quantities for the same year (2038) obtained from the ONS 2014-based NPP. For most of the age range, the forecasts are similar, with the principal projection falling close to the median prediction under the GAM-based model. However, the ONS model projects lower mortality for young adults for both sexes, to the extent that the principal projections fall outside the outermost 90% predictive interval of the probabilistic projections. This is due to a

greater weight that is given by the ONS methodology to more recent high improvement rates at these ages (see Office for National Statistics (2016) for more details regarding the ONS methodology).

9.1. Life expectancy

Period life expectancy at birth is a useful summary measure of the mortality conditions in a given year. It captures the expected number of years lived of a hypothetical individual who experiences a given period's schedule of mortality rates over the course of their whole life. Fig. 14 compares the posterior distribution of life expectancy at birth, e_0 , from the jointly fitted GAM-based model with the equivalent quantity from the NPP. The GAM-based forecasts appear more optimistic than the ONS equivalent, with median life expectancy higher than the principal ONS projection because of the lower predictions of mortality at ages 70–95 years under the GAM-based model. Fig. 14 also reveals that uncertainty in e_0 initially grows more quickly in the Bayesian approach that was developed above, in that the gap between the high and low variants is much narrower than the fan intervals for at least the first decade of the forecast. After 30 years, however, the range that is spanned by the ONS variants becomes wider than the 90% probabilistic interval from the GAM-based model. The uncertainty in the probabilistic forecast reflects past variability in the observed data and, from the comparison with hold-back data given in Figs 11 and 12, the calibration of this uncertainty appears reasonable. As a result, we believe that the probabilistic intervals provide a better indication of the uncertainty around future life expectancy than the scenario-based equivalents, at least in the short term, particularly as they have a readily understandable interpretation in terms of probability.

10. Discussion and conclusion

This paper details methodology for the fully probabilistic forecasting of mortality rates, accounting for uncertainty in parameter estimates as well as in forecasting. The approach uses a GAM to produce smooth rate estimates at younger ages and combines this with a parametric model at higher ages where the data are more sparse, allowing rate estimates to be obtained for extreme old ages. The use of Hamiltonian Monte Carlo sampling and the *stan* software package allowed posterior sampling to be conducted with reasonable efficiency.

Stacking predictive distributions following the approach of Yao *et al.* (2018) provides a principled approach to avoiding a single choice of transition point between these two submodels governing younger and older age ranges. These weights are based on approximate leave-one-out cross-validation performance and thus weight models on the basis of their ability to predict data that are contained in the original fitting period. An alternative approach may be to fit models on a subset of data, and to produce weights based on model performance in forecasting data at the end of the time period. However, this would involve additional model refitting, and it may also be that such assessments are overly sensitive to characteristics of the held-out data. Furthermore, log-scores based on a single set of observed outcomes are likely to be highly correlated, and thus rolling n -step-ahead forecasts may be required to assess forecast performance robustly, which would necessitate repeated model fitting with even greater computational expense.

A comparison with ONS forecasts provides an indication of how Bayesian predictive intervals compare with the deterministic scenario-based indicators of forecast variability that are produced by the ONS. For life expectancy in particular, the probabilistic intervals are considerably wider over a short time horizon than those suggested by the high and low mortality scenarios.

Future work could investigate the inclusion of expert opinion in probabilistic mortality forecasting models like that presented in this paper. The NPP uses experts to provide target rates of mortality improvement over longer time horizons (25 years) (Office for National Statistics, 2016), reflecting the fact that extrapolative methods may prove inferior to expertise at this distance into the future. A similar approach within a Bayesian framework would have to consider that using expert opinion about future rates is different from the standard approach of eliciting information about model parameters directly. Work in Dodd *et al.* (2018b) describes one way in which this could be achieved. Beyond this, there are also opportunities to investigate the possibility of extending similar methods to other demographic components, particularly fertility.

Acknowledgements

This work was supported by the Economic and Social Research Council Centre for Population Change—phase II (grant ES/K007394/1) and a research contract to review the methodology for projecting mortality between the ONS and the University of Southampton. The use of the IRIDIS High Performance Computing Facility, and associated support services at the University of Southampton, in the completion of this work is also acknowledged. Earlier work on this model was presented at a joint Eurostat–United Nations Economic Commission for Europe work session on demographic projections (Forster *et al.*, 2016). All the views presented in this paper are those of the authors only.

References

- Beard, R. (1963) A theory of mortality based on actuarial, biological, and medical considerations. In *Proc. Int. Population Conf.*, pp. 611–625. New York: International Union for the Scientific Study of Population.
- Brouhns, N., Denuit, M. and Vermunt, J. K. (2002) A Poisson log-bilinear regression approach to the construction of projected lifetables. *Insur. Math. Econ.*, **31**, 373–393.
- Cairns, A. J. G., Blake, D., Dowd, K., Coughlan, D., Epstein, D. and Ong, A. (2009) A quantitative comparison of stochastic mortality models using data from England and Wales and the United States. *Nth Am. Act. J.*, **13**, 1–35.
- Continuous Mortality Investigation (2016) CMI mortality projections model consultation. *Working Paper 90*. Institute and Faculty of Actuaries, London. (Available from <https://www.actuaries.org.uk/documents/cmi-working-paper-90-cmi-mortality-projections-model-consultation>.)
- Currie, I. D., Durban, M. and Eilers, P. H. C. (2004) Smoothing and forecasting mortality rates. *Statist. Modelling*, **4**, 279–298.
- Dodd, E., Forster, J. J., Bijak, J. and Smith, P. W. F. (2018a) Smoothing mortality data: the *English Life Tables*, 2010–2012. *J. R. Statist. Soc. A*, **181**, 717–735.
- Dodd, E., Forster, J. J., Bijak, J. and Smith, P. W. F. (2018b) Stochastic modelling and projection of mortality improvements using a hybrid parametric/semiparametric age-period-cohort model. University of Southampton, Southampton. (Available from <https://eprints.soton.ac.uk/42219/>.)
- Dowd, K., Cairns, A. J. G., Blake, D., Coughlan, G. D., Epstein, D. and Khalaf-Allah, M. (2010) Evaluating the goodness of fit of stochastic mortality models. *Insur. Math. Econ.*, **47**, 255–265.
- Forster, J. J., Dodd, E., Bijak, J. and Smith, P. W. F. (2016) A comprehensive framework for mortality forecasting. *Jt Eurostat–United Nations Economic Commission for Europe Work Session Demographic Projections*, Geneva.
- Gelman, A., Carlin, J. B., Stern, H. S., Dunson, D. B., Vehtari, A. and Rubin, D. B. (2014) *Bayesian Data Analysis*, 3rd edn. Abingdon: CRC Press.
- Gelman, A. and Rubin, D. B. (1992) Inference from iterative simulation using multiple sequences. *Statist. Sci.*, **7**, 457–472.
- Giroi, F. and King, G. (2008) *Demographic Forecasting*. Princeton: Princeton University Press.
- Hoffman, M. D. and Gelman, A. (2014) The no-U-turn sampler: adaptively setting path lengths in Hamiltonian Monte Carlo. *J. Mach. Learn. Res.*, **15**, 1–31.
- Human Mortality Database (2018) Human mortality database. Max Planck Institute for Demographic Research, Rostock. (Available from <http://www.mortality.org>.)
- Hyndman, R. J. and Ullah, M. S. (2007) Robust forecasting of mortality and fertility rates: a functional data approach. *Computat. Statist. Data Anal.*, **51**, 4942–4956.

- Keyfitz, N. and Caswell, H. (2005) *Applied Mathematical Demography*, 3rd edn. New York: Springer.
- Lang, S. and Brezger, A. (2004) Bayesian P-splines. *J. Computat Graph. Statist.*, **13**, 183–212.
- Lee, R. D. and Carter, L. R. (1992) Modeling and forecasting U.S. mortality. *J. Am. Statist. Ass.*, **87**, 659–671.
- Møller, B., Fekjær, H., Hakulinen, T., Sigvaldason, H., Storm, H. H., Talbäck, M. and Haldorsen, T. (2003) Prediction of cancer incidence in the Nordic countries: empirical comparison of different approaches. *Statist. Med.*, **22**, 2751–2766.
- Neal, R. (2010) MCMC using Hamiltonian Dynamics. In *Handbook of Markov Chain Monte Carlo* (eds S. Brooks, A. Gelman, G. Jones and X.-L. Meng). Boca Raton: Chapman and Hall–CRC.
- Office for National Statistics (2016) National population projections: 2014-based reference volume, series PP2. *Technical Report*. Office for National Statistics, Newport. (Available from <https://www.ons.gov.uk/peoplepopulationandcommunity/populationandmigration/populationprojections/compendium/nationalpopulationprojections/2014basedreferencevolumeseriespp2>.)
- Palin, J. (2016) When is a cohort not a cohort?: Spurious parameters in stochastic longevity models. In *Proc. Int. Mortality and Longevity Symp.* London: Institute and Faculty of Actuaries.
- R Core Team (2017) *R: a Language and Environment for Statistical Computing*. Vienna: R Foundation for Statistical Computing.
- Renshaw, A. and Haberman, S. (2003a) Lee–Carter mortality forecasting with age-specific enhancement. *Insur. Math. Econ.*, **33**, 255–272.
- Renshaw, A. and Haberman, S. (2003b) Lee–Carter mortality forecasting: a parallel generalized linear modelling approach for England and Wales mortality projections. *Appl. Statist.*, **52**, 119–137.
- Renshaw, A. and Haberman, S. (2006) A cohort-based extension to the Lee–Carter model for mortality reduction factors. *Insur. Math. Econ.*, **38**, 556–570.
- Richards, S. J., Currie, I. D., Kleinow, T. and Ritchie, G. P. (2017) A stochastic implementation of the APCI model for mortality projections. *Sessional Research Paper*. Actuarial Research Centre, Institute and Faculty of Actuaries, London. (Available from <https://www.actuaries.org.uk/documents/stochastic-implementation-apci-model>.)
- Stan Development Team (2015) *Stan Modeling Language Users Guide and Reference Manual*.
- Thatcher, A. F., Kannisto, V. and Vaupel, J. W. (1998) *The Force of Mortality at Ages 80–120*. Odense: Odense University Press.
- Vaupel, J. W., Manton, K. G. and Stallard, E. (1979) The impact of heterogeneity in individual frailty on the dynamics of mortality. *Demography*, **16**, 439–454.
- Vehtari, A., Gelman, A. and Gabry, J. (2016) Practical Bayesian model evaluation using leave-one-out cross-validation and WAIC. *Statist. Comput.*, **27**, 1–20.
- Willeits, R. C. (2004) The cohort effect: insights and explanations. *Br. Act. J.*, **10**, 833–877.
- Wilmouth, J. R., Andreev, K., Jdanov, D., Gleij, D. A. and Riffe, T. (2017) Methods protocol for the human mortality database. *Technical Report*. Human Mortality Database. (Available from <http://www.mortality.org/Public/Docs/MethodsProtocol.pdf>.)
- Wiśniowski, A., Smith, P. W. F., Bijak, J., Raymer, J. and Forster, J. J. (2015) Bayesian population forecasting: extending the Lee–Carter method. *Demography*, **52**, 1035–1059.
- Wood, S. N. (2006) *Generalised Additive Models: an Introduction with R*. Boca Raton: Chapman and Hall–CRC.
- Wood, S. N. (2016) Just another Gibbs additive modeller: interfacing JAGS and mgcv. *arXiv Preprint*. University of Bath, Bath. (Available from <http://arxiv.org/abs/1602.02539>.)
- Yao, Y., Vehtari, A., Simpson, D. and Gelman, A. (2018) Using stacking to average Bayesian predictive distributions. *Bayes Anal.*, to be published.

Supporting information

Additional ‘supporting information’ may be found in the on-line version of this article:

‘Appendix: Constructing prior distributions conditional on constraints’.